A membrane-associated movement protein of *Pelargonium flower break virus* shows RNA-binding activity and contains a biologically relevant leucine zipper-like motif

Sandra Martínez-Turiño, Carmen Hernández*

Instituto de Biología Molecular y Celular de Plantas (Consejo Superior de Investigaciones Científicas-Universidad Politécnica de Valencia). Ciudad Politécnica de la Innovación, Ed. 8E. Camino de Vera s/n, 46022 Valencia, Spain

* Corresponding author. Mailing address: Carmen Hernández, Instituto de Biología Molecular y Celular de Plantas, (CSIC-Universidad Politécnica de Valencia). Ciudad Politécnica de la Innovación, Ed. 8E. Camino de Vera s/n, 46022 Valencia, Spain. Phone: 34-96-3877869   Fax: 34-96-3877859 E-mail: cahernan@ibmcp.upv.es

1

1 **ABSTRACT**

2   Two small viral proteins (DGBp1 and DGBp2) have been proposed to act in a

3 concerted manner to aid intra- and intercellular trafficking of carmoviruses though the

4 distribution of functions and mode of action of each protein partner are not yet clear.

5 Here we have confirmed the requirement of the DGBps of *Pelargonium flower break*

6 *virus* (PFBV), p7 and p12, for pathogen movement. Studies focused on p12 have shown

7 that it associates to cellular membranes, which is in accordance to its hydrophobic

8 profile and to that reported for several homologs. However, peculiarities that distinguish

9 p12 from other DGBps2 have been found. Firstly, it contains a leucine zipper-like motif

10 which is essential for virus infectivity in plants. Secondly, it has an unusually long and

11 basic N-terminal region that confers RNA binding activity. The results suggest that

12 PFBV p12 may differ mechanistically from related proteins and possible roles of PFBV

13 DGBps are discussed.

14

15   *Key words*: Carmovirus; PFBV; Movement proteins; RNA-binding domain; Leucine

16 zipper-like motif; Membrane association; Subcellular localization.

1 Introduction

2   To establish a productive infection, plant viruses need to move from their replication

3   sites to and through plasmodesmata (PD), which are wall spanning co-axial

4   membranous organelles that bridge the cytoplasm of contiguous cells (Benítez-Alfonso

5   et al., 2010). Such intracellular and intercellular pathogen trafficking can take place in

6   the form of viral particles or nucleoprotein complexes and depends on virus encoded

7   polypeptides named movement proteins (MPs). Though there is considerable structural

8   diversity among MPs of distinct virus taxa (Lucas, 2006), functional properties common

9   to most of them can be outlined including nucleic acid binding capacity, interaction

10   with viral and host factors and ability to increment the size exclusion limit of PD

11   (Nelson and Citovsky, 2005; Waigmann et al., 2004). As viruses seem to hijack the

12   cellular machinery of macromolecular transport to promote their own movement, MPs

13   also often associate with host membrane or cytoskeletal elements (Harries et al., 2010).

14   All these activities can be combined in a single MP or be allocated to several MPs that

15   will assist virus spread in a concerted manner (Hull, 2002; Lucas, 2006).

16   *Pelargonium flower break virus* (PFBV) is a member of the genus *Carmovirus* in

17   the family *Tombusviridae*. The monopartite single-stranded (ss) RNA genome of PFBV

18   contains five ORFs that encode polypeptides of 27 (p27), 86 (p86), 7 (p7), 12, (p12) and

19   37 (p37) kDa (Rico and Hernández, 2004). Reverse genetics experiments have indicated

20   that p27 and its readthrough product p86 (the RNA dependent-RNA polymerase), are

21   essential for viral RNA replication while p37 plays a dual role as capsid protein and as

22   suppressor of RNA silencing (Martínez-Turiño and Hernández, 2009, 2010). According

23   to the available data, cell-to-cell transport of carmo-like viruses in plants is aided by two

24   small virus-encoded polypeptides referred to as the double gene block proteins (DGBps;

1   Hull, 2002). In the case of PFBV, DGBp1 and DGBp2 would correspond to p7 and p12,

2   respectively, on the basis of their similarities with carmoviral proteins with assigned

3   movement function (Genovés et al., 2006; Hacker et al., 1992; Li et al., 1998).

4   Structural and molecular studies performed with *Carnation mottle virus* (CarMV) and

5   *Melon necrotic spot virus* (MNSV) have shown that their DGBps1 (CarMV p7 and

6   MNSV p7A) present RNA binding properties mainly mediated by a basic central region

7   that adopts an α-helical conformation in the presence of secondary structure inducers

8   (Marcos et al., 1999; Navarro et al., 2006; Vilar et al., 2001, 2005). Conversely,

9   DGBps2 of these viruses lack RNA binding activity and contain one (MNSV p7B) or

10   two (CarMV p9) transmembrane domains (TMs) that are targeted and inserted *in vitro*

11   into microsomal membranes derived from the endoplasmic reticulum (ER) (Navarro et

12   al., 2006; Vilar et al., 2002). From these findings, a topological model was advanced in

13   which the cytosolic faced-region(s) of the membrane-associated movement protein

14   (DGBp2) would interact with the soluble partner (DGBp1) bound to the viral RNA

15   through their C-terminal regions that might adopt similar β-sheet structures (Navarro et

16   al., 2006; Vilar et al., 2002). The resulting ribonucleotide complex would spread among

17   cells with the aid of an internal membranous translocation system, paralleling that

18   proposed for other MPs (Heinlein and Epel, 2004; Lucas, 2006; Melcher, 2000; Nelson

19   and Citovsky, 2005). As indicated above, this model was mainly based on the properties

20   of DGBps of CarMV and MNSV but *in silico* analyses of the corresponding proteins of

21   other carmoviruses revealed common features that led to the suggestion that the model

22   could apply for most members of the genus (Navarro et al., 2006). Though this was an

23   attractive and straightforward scheme, the mechanism for carmoviral movement is

24   likely more complex and, moreover, virus-specific particularities cannot be discarded.

25   Indeed, most recent results with the DGBps of MNSV have shown that MNSV p7B is

1 targeted *in vivo* to the ER as expected, and delivered to PD via a route that involves the

2 Golgi apparatus (Genovés et al., 2010). However, MNSV p7A is not only able to bind

3 RNA but also to move intracellularly toward PD in the absence of other viral products

4 through a route distinct from that followed by p7B (Genovés et al., 2009). This

5 observation suggests that the distribution of functions among DGBp partners is different

6 or not so well defined as initially proposed.

7   PFBV p12, like its counterparts in other carmoviruses, contains a high percentage of

8 hydrophobic amino acids distributed along two predicted transmembrane α-helices

9 (Navarro et al., 2006). This trait probably causes the protein to become membrane

10 embedded as described for the homologous CarMV and MNSV proteins and lately for

11 that of *Turnip crinkle virus* (TCV) (Martínez-Gil et al., 2010; Navarro et al., 2006; Vilar

12 et al., 2002). However, several structural peculiarities distinguish PFBV p12 from

13 similar proteins. First, its size is bigger than those of equivalent carmoviral proteins

14 that, with the only exception of the putative DGBp2 of *Japanese iris necrotic ring virus*

15 (Takemoto et al., 2000), range from 7 to 9 kDa (Lommel et al., 2005). Alignment of

16 PFBV p12 with the latter ones indicates that this size gain is primarily due to an N-

17 terminal extension which is rich in basic amino acids (Rico and Hernández, 2004). In

18 addition, p12 contains a seven residue leucine repeat motif, consistent with a leucine

19 zipper, that is absent in related proteins and that is predicted to be four heptads in length

20 (Rico and Hernández, 2004). The natural heterogeneity found among different PFBV

21 isolates argues in favor of the functional relevance of the motif. On one side, only

22 conservative amino acid changes were detected in this region of the molecule and the

23 key leucines of the heptads were strictly preserved despite the large nucleotide variation

24 observed in the corresponding codons (Rico et al., 2006). In addition, an amino acid

1 substitution observed in one isolate would extend the number of heptads of the motif

2 from four to five (Rico et al., 2006).

3   In order to get insights into the mode of action of PFBV p12, in this work we report

4 experiments aimed at confirming its involvement, together with PFBV p7, in viral

5 movement. We have also investigated the subcellular localization of the protein and the

6 relevance *in vivo* of the putative leucine zipper. Moreover, we have tested whether p12

7 is endowed with RNA binding activity. Collectively, the results suggest that PFBV p12

8 may differ mechanistically from related proteins.

9 **Results**

10 *Both p7 and p12 are involved in PFBV cell to cell movement*

11   In order to assess whether the two small polypeptides encoded in the central region

12 of PFBV genome, p7 and p12, are involved in viral movement as expected from their

13 homologies with carmoviral proteins of known function (Genovés et al., 2006; Hacker

14 et al., 1992), the start codons of their corresponding ORFs were altered by site-directed

15 mutagenesis using the PFBV infectious clone pSP18F-IC (Rico and Hernández, 2006)

16 as template (Fig. 1A). Run-off transcripts synthesized from the wild type (wt) and the

17 mutated constructs, designated p7aug- and p12aug-, respectively, were used to inoculate

18 *Chenopodium quinoa* leaves and protoplasts. Unlike that observed with the wt

19 construct, no lesions were visible in leaves challenged with the mutant constructs even

20 at 15 days post-inoculation (dpi) and, consistently, no viral-specific signals could be

21 detected by Northern blot hybridization (Fig. 1B). In contrast to that found in plants,

22 mutants p7aug- and p12aug- accumulated in *C. quinoa* protoplasts at levels similar to

23 those of the wt RNA (Fig. 1B). Collectively, the results showed that abolishment of p7

1 or p12 expression does not affect viral replication but impairs viral spread in leaves

2 supporting the anticipated role of these proteins in cell-to-cell movement.

3 *Amino acid mutations in the leucine zipper-like motif of p12 render movement-defective*

4 *viruses*

5   To investigate the *in vivo* relevance of the leucine zipper-like motif of p12,

6 nucleotide substitutions leading to single or double replacements of heptadic leucine

7 residues were engineered into the infectious clone pSP18-IC. The mutations affected

8 either Leu67 (mutants LZM1 and LZM2 with the amino acid substitutions Leu67Ile and

9 Le67Ala, respectively), Leu81 (mutants LZM3 and LZM4 with the amino acid

10 substitutions Leu81Arg and Leu81Ala, respectively), or both simultaneously (mutants

11 LZM5, with changes Leu67Ile and Leu81Arg, and LZM6, with changes Leu67Ala and

12 Leu81Ala) (Fig. 2A). The replacement Leu67 by Ile and Leu81 by Arg was based on

13 the presence of such amino acid residues at equivalent positions of homologous proteins

14 (Rico and Hernández, 2004). On the other hand, Ala was chosen over other amino acids

15 as a substituting residue of the heptadic leucine residues because of the fact that Ala has

16 a strong propensity to form an α-helix and its substitution has been documented to have

17 minimal disruptive effects on the alpha-helical structure characteristic of a leucine

18 zipper domain (Lyu et al., 1990; O´Neil and DeGrado, 1990; Zhang et al., 1991). In

19 addition, Ala lacks the bulky hydrophobic side chain of a leucine residue, which is

20 believed to be the major hydrophobic force for a leucine zipper domain to facilitate

21 protein interaction (O´Shea et al., 1989). Thus, replacement of heptadic leucine residues

22 by alanine would likely influence only the biological properties derived from the bulky

23 hydrophobic side chain of a leucine residue while having minimal effects on the overall

24 alpha-helical structure. Transcripts derived from the wt and mutant clones were used to

1   inoculate *C. quinoa* plants. As opposed to wt RNA, none of the mutants induced

2   appearance of chlorotic lesions on the inoculated leaves and a Northern blot analysis

3   confirmed the absence of PFBV in this plant material (Fig. 2B, upper panel). Two

4   control mutants were additionally generated, one with the putative leucine zipper

5   extended in one heptad (change Ser53Leu) and the other harbouring an amino acid

6   replacement outside of the leucine zipper-like motif (Gly14Glu) as found, respectively,

7   in one and nineteen natural isolates of the virus (Rico et al., 2006). These mutants were

8   fully infectious in *C. quinoa* (data not shown) denoting that the results observed through

9   alteration of critical residues of the leucine zipper motif were sequence-specific and not

10   a side effect of the mutagenesis. In order to eliminate the possibility that the nucleotide

11   substitutions engineered in constructs LZM1 to LZM6 disrupted *cis*-acting elements

12   essential for replication, these constructs were transfected in *C. quinoa* protoplasts.

13   Northern blot analysis revealed that all assayed mutants accumulated to levels

14   equivalent to those of the wt RNA (Fig. 2B, lower panel), indicating that their

15   incapacity to establish effective infections in plants was due to a defect in movement

16   rather than to a blockage in viral replication. Overall, the data support the conclusion

17   that the leucine zipper-like motif is critical for the movement function of p12.

18   *p12 mainly localizes to the ER and is recovered in membranous fractions*

19   As indicated above, computer analysis of p12 sequence predicted that it is a

20   membrane protein with two TMs that roughly span from residues 25 to 50 and 60 to 82,

21   respectively (Fig. 2A). To investigate potential association of p12 to cellular

22   membranes, this PFBV product was fused to the green fluorescent protein (GFP) and

23   transiently expressed in *Nicotiana benthamiana* leaves via agroinfiltration. Whereas

24   expression of free GFP gave the typical diffuse green fluorescence evenly distributed

1 through the cytoplasm and the nucleus, fluorescence derived from the fusion p12GFP

2 labelled an intracellular reticulate network likely corresponding to the ER (Fig. 3, panels

3 A and B). To confirm this issue, p12 was fused to the monomeric red fluorescent

4 protein (mRFP) and delivered by agroinfiltration into transgenic 16c *N. benthamiana*

5 plants expressing ER-targeted GFP (GFP-KDEL, Ruiz et al., 1998). A perfect match

6 among the p12mRFP and GFP-KDEL fluorescent signals was observed thus

7 corroborating that p12 localizes mainly to the ER (Fig. 3, panels D to F). Nevertheless,

8 sorting of the protein to other cellular membranes cannot be excluded since the green

9 fluorescence of the p12GFP fusion was occasionally observed in punctuate structures at

10 the cytoplasm and close to the plasma membrane (Fig. 3, panel C and data not shown).

11 Interestingly, the pattern of cytoplasmic punctuate structures strongly resembled the

12 motile bodies formed by MNSV p7b at the Golgi stacks (Genovés et al., 2010).

13 Consistent with these general observations, subcellular fractionation and Western blot

14 analysis of proteins extracted from GFP- and p12GFP-expressing plant tissue revealed

15 the presence of the fused product in the pellet fraction (P30) following centrifugation at

16 30.000 x g, in contrast to the unfused GFP that, as expected, was recovered in the

17 supernatant (S30) (Fig. 3G). Because the P30 fraction contains membrane-derived

18 microsomes, we can conclude that p12 is indeed a membrane-associated protein.

19 *p12 has RNA binding activity*

20 Positively charged amino acids are frequently involved in nucleic acid binding

21 properties of proteins (Chen and Varani, 2005; Weiss and Narayana, 1998). As

22 mentioned previously, PFBV p12 contains a specific N-terminal extension which is rich

23 in basic amino acids (Fig. 2A). This structure prompted us to explore whether this

24 protein could be endowed with RNA binding activity, which would differ from that

reported for the equivalent product of MNSV or postulated for other DGBps2 (Navarro et al., 2006; Saurí et al., 2005). To this aim, a recombinant p12 fused to a His-tag was expressed in *E. coli* and purified by chromatography on Ni-NTA columns. Despite the known difficulties associated to production and purification of hydrophobic, membrane proteins in bacteria (Luan et al., 2004), we were able to obtain sufficient amounts for biochemical studies. In order to improve protein solubility, Arg and Glu were added at 50 mM to the storage buffer which had a positive effect in preventing protein aggregation and precipitation and increased the long-term stability of the sample, in line with that described for diverse proteins (Golovanov et al., 2004). Electrophoretic mobility shift assays (EMSAs) were performed with increasing quantities of the recombinant protein and a ^{32}P-labeled ssRNA probe (5′-PFBV) encompassing the 5′-terminal 140 nt of PFBV genome. RNA mobility shift, suggesting the presence of an RNA protein-interaction, became detectable when the His-tagged p12 was added at a concentration of 0.21 μM to the reaction mixture. Complete retardation of the probe was observed at 13.10 μM and at higher concentrations, as measured by disappearance of unbound RNA (Fig. 4A). Treatment of the preparation of purified p12 with proteinase K before adding the RNA probe prevented formation of the retarded band confirming that the shift resulted from the interaction of the RNA with the protein (data not shown). Furthermore, when the His-tagged p12 was replaced by bovine serum albumin (BSA) in control gel shift assays, no retardation of the probe was observed indicating that the association between p12 and the ssRNA was not an artefact of the specific experimental conditions employed (Fig. 4A, lane 10). Non-linear regression of the binding data (Fig. 4B) allowed estimating an apparent K_d of 3.14 μM, which was in the range of those reported for distinct viral RNA binding proteins including several MPs (Daròs and Carrington, 1997; Herranz and Pallás, 2004; Marcos et al., 1999; Navarro et al., 2006;

Skuzeski and Morris, 1995). Only two forms of the probe were detectable in the EMSA assays, free RNA and completely retarded complex with no obvious intermediate shifted bands, which would suggest a cooperative binding of p12 to ssRNA (Citovsky et al., 1990). However, the slope of the best-fit curve (h or Hill slope) for the binding data, calculated from three independent experiments, was found to be 1 lending little support to a cooperative view of the protein:RNA interaction ($h=1$ is indicative of non-cooperative binding and $h>1$ is an indication of positive cooperative binding). It is worth mentioning in this context that attempts to further concentrate our protein preparation without affecting stability were unsuccessful, which precluded more detailed characterization of the binding kinetics.

To investigate how the RNA-binding ability of p12 was dependent on electrostatic interactions, EMSAs were performed using increasing NaCl concentrations in the incubation mixtures. An amount of protein that was sufficient to bind all RNA molecules was employed (40.0 µM) and, thus, the appearance of free RNA was quantified to evaluate complex dissociation (Fig. 4C). The NaCl concentration at which binding was reduced to 50% of maximal levels (IC_{50}) was 525 mM, a remarkable salt tolerance that, nevertheless, was in the range of those determined for other RNA-binding proteins of viral origin (Brantley and Hunt, 1993; López et al., 2000; Marcos et al., 1999; Martínez-Turiño and Hernández, 2010; Navarro et al., 2006; Richmond et al., 1998). These results suggested that electrostatic interactions are not the only ones involved in binding of p12 to the RNA.

p12 is a non-sequence specific ssRNA binding protein

Competition experiments were performed to examine the binding selectivity of p12. For this purpose, unlabeled nucleic acids corresponding to either ssRNA, double-

1   stranded (ds) RNA, ssDNA or dsDNA molecules were added to the binding mixtures at

2   1-, 10- and 100-fold molar excess over the radiolabeled probe. In the case of ssRNA,

3   two distinct competitors were used, one derived from the 3′-terminal region of the

4   PFBV genome (3′PFBV-ssRNA) and the other from a heterologous source (het-

5   ssRNA). Fixed amounts of His-tagged p12 (32.75 μM) and ^{32}P-labeled 5-PFBV probe

6   (97.0 pM), that resulted in more than 99 % of the ssRNA bound to the protein, were

7   used in the binding reactions. EMSAs revealed that dsRNA and dsDNA were poor

8   competitors because a major fraction of the probe remained bound to p12 even at a 100

9   molar excess (Fig. 5). At the same molar excess, the ssDNA behaved as moderately

10   good competitor as the binding of p12 to the probe was significantly affected (Fig. 5).

11   However, ssRNAs were undoubtedly the best competitors irrespectively of their origin,

12   as they completely prevented formation of the p12:probe complex when added at the

13   greatest concentration (Fig. 5). Overall, the data indicated that p12 is a single-stranded

14   nucleic acid-binding protein with the highest preference toward any ssRNA.

15   *p12 RNA binding is attributable to its basic N-terminal domain*

16   In order to map the region of p12 responsible of its binding activity, the N- or C-

17   terminal region of the molecule was removed to create two truncated forms of the

18   protein, p12(26-106) and p12(1-59). In addition, several mutated versions of p12(1-59)

19   were generated by consecutively replacing Arg residues of the N-terminal region by

20   Ala. The mutants were designated as p12(1-59)m2R (carrying substitutions Arg16Ala

21   and Arg17Ala), p12(1-59)m3R (carrying substitutions Arg16Ala, Arg17Ala and

22   Arg19Ala) and p12(1-59)m4R (carrying substitutions Arg16Ala, Arg17Ala, Arg19Ala

23   and Arg24Ala) (Fig. 6A). All p12 derivatives were expressed in *E. coli* as His-tagged

24   fusions, purified by chromatography on Ni-NTA columns and subjected to

1   Northwestern assay to evaluate RNA-binding capability. To this aim, equivalent

2   amounts of the purified proteins were separated, together with the wt p12, by SDS-

3   PAGE and subsequently transferred to a nitrocellulose membrane. After a renaturation

4   step, the membrane was incubated with ^{32}P-labeled 5′-PFBV ssRNA probe. A signal

5   was detected in the position corresponding to the full-length protein (Fig. 6B) which

6   was in accordance with the EMSA results and ruled out the possibility that any

7   contaminating protein(s) from *E. coli* could account for the observed RNA binding

8   activity. Remarkably, a similar, or even stronger, signal was noticed in the position of

9   p12(1-59) whereas no signal was present in the portion of the membrane that contained

10 p12(26-106). These results strongly suggested that the RNA binding properties of p12

11 could be provided by its N-terminal basic extension. Consistent with this possibility,

12 double replacement of Arg by Ala in this domain strongly diminished the binding

13 capability of p12(1-59) (protein p12[1-59]m2R; Fig. 6B) which was reduced to

14 negligible levels when one or two additional Arg residues were mutated (proteins

15 p12[1-59]m3R and p12[1-59]m4R, respectively; Fig. 6B). These results confirmed the

16 involvement of the N-terminal region in the binding activity of p12 and, moreover,

17 highlighted the contribution of positively charged amino acids to such activity.

18 **Discussion**

19   Here, we have corroborated the requirement of the two small, centrally encoded

20 PFBV proteins, p7 and p12, for virus movement. Computer analyses suggest that PFBV

21 p7 structure fits well with the general scheme proposed for carmoviral DGBp1 that

22 distinguishes three different structural domains: an unordered N-terminus, an α-helical

23 central region and a C-terminus with potential β-sheet folding (Akgoz et al., 2001;

24 Marcos et al., 1999; Navarro et al., 2006; Vilar et al., 2001, 2005). The central region is

1   rich in positively charged amino acids and is expected to endow the protein with RNA

2   binding properties as it has been demonstrated for CarMV and MNSV DGBp1 (Marcos

3   et al., 1999; Navarro et al., 2006) as well as the corresponding product of *Turnip crinkle*

4   *virus* (Wobbe et al., 1998). According to *in silico* evaluations, PFBV p12 shares also

5   main features with related products including a C-terminal region with likely β-sheet

6   folding and the presence of two transmembrane domains. Consistent with the latter

7   prediction, the protein was recovered in membranous fractions and it was found to

8   localize mainly to the ER, paralleling that reported for homologous and non-

9   homologous MPs (Genovés et al., 2010; Heinlein et al., 1998; Ju et al., 2005;

10   Peremyslov et al., 2004; Schepetilnikov et al., 2008). Nevertheless, as PD is most

11   probably the final target of p12, interaction of the protein with other components of the

12   cellular macromolecular transport system at different stages of infection cannot be ruled

13   out. This possibility was indeed suggested by some localization patterns of p12 (Fig. 3,

14   panel C and data not shown) and, if confirmed, it would be in line with that reported for

15   MNSV p7B and for distinct MPs (Genovés et al., 2010; Haupt et al., 2005; Heinlein et

16   al., 1998). Despite the above similarities, PFBV p12 differs from other carmoviral

17   DGBps2 in having a basic N-terminal extension and a leucine zipper-like motif. This

18   prompted us to investigate potential functional implications of these PFBV p12-

19   particular traits.

20   Leucine zippers are know to engage in protein-protein interactions and are

21   composed of a heptad repeat of amino acids (Busch and Sassone-Corsi, 1990;

22   Landschultz et al., 1988). This type of motifs adjust frequently to the "abcdefg rule" that

23   holds that positions "a" and "d" of the heptad are occupied by hydrophobic amino acids

24   while positions "e" and "g" are occupied by charged amino acids. Though this rule is

25   usually met by "classical" leucine zipper motifs, numerous modified leucine zippers that

1 show lax adherence to the rule but preserve their function as intermolecular clamps have

2 been described (e.g: Chevalier et al., 2008; Fry et al., 1999). In many cases, however,

3 the presence of leucine residues at positions "d" has been found to be critical (Bornberg-

4 Bauer et al., 1998; Moitra et al., 1997). The putative leucine zipper of PFBV p12

5 deviates to some extent from the classical structure (Fig. 2) but the strict conservation of

6 the motif and, particularly, of the key leucines in all isolates of the virus characterized

7 so far (Rico et al., 2006) suggested it could be relevant for the functionality of the

8 protein. Supporting this view, single and double alterations of pivotal leucines rendered

9 p12 mutants unable to aid viral movement. Most likely, the engineered amino acid

10 substitutions precluded essential association(s) of p12 with itself and/or with proteins of

11 distinct nature. The involvement of leucine zipper motifs in homo and/or

12 heterodimerization has been reported in both animal and plant viruses. Examples of the

13 latter ones include the interaction between the aphid transmission factor and the virion-

14 associated protein of *Cauliflower mosaic virus* (Leh et al., 1999), or the self-interaction

15 of the ORF II-encoded product of *Soybean chlorotic mottle virus* (Takemoto and Hibi,

16 2005). We have tried to search for p12 interacting proteins through the split-ubiquitin

17 membrane two-hybrid assay (Fetchko and Stagljar, 2004) but our attempts have been

18 unsuccessful as p12 used as bait caused activation of the reporter in the absence of prey

19 proteins. Assessment of potential p12 homodimerization through bimolecular

20 fluorescence complementation (BiFC) has neither yielded clear results (data not shown).

21 Other approaches will be needed to investigate formation of hydrophobic bonds among

22 the leucine zipper of p12 and other leucine zipper partners. Interestingly, a host

23 homeodomain leucine zipper protein has been found to interact with the MP of a related

24 virus, *Tomato bushy stunt virus* (genus *Tombusvirus*, family *Tombusviridae*), an

25 interaction that correlated with the movement activity of the protein (Desvoyes et al.,

2002). Whether this factor and/or different ones are recruited by p12 for directing viral

transport remains to be seen. It is also worth mentioning that leucine zippers have been

implicated in some instances in regulation of post-translational modification(s) rather

than in promotion of protein-protein interactions (Long et al., 2008; Pagano et al.,

2009). Such type of modifications might play an important role in MP activity

(Kawakami et al., 2003). Several phosphorylation and glycosylation sites are predicted

in p12 (data not shown). We can thus not exclude that mutations introduced in its

leucine zipper-like motif have not a direct effect on association of the protein with

specific viral/host factors but instead provoke conformational changes that prevent post-

translational modifications required for modulation of its activity.

The other peculiarity of PFBV DGBp2 concerns to its size increment when

compared with homologous proteins, an increment that results from the presence of an

N-terminal extension. Abolishment of the initiation codon of ORF p12 in mutant

p12aug- might still allow translation from the downstream ^{2424}AUG which would led to

production of a truncated protein with a predicted size (8.5 kDa) resembling more those

of other DGPps2 (Navarro et al., 2006). The lack of infectivity of this mutant in plants

supports that the N-terminus of p12 is absolutely required during the virus life cycle.

Outstandingly, we have shown that, unlike related proteins, PFBV p12 possesses RNA

binding activity and, moreover, that this activity is provided by its N-terminal region.

Basic residues of this region have been shown to play an essential role in RNA binding

as mutation of just two arginine residues strongly reduced the capability of the protein

to interact with the RNA and this capability was virtually abolished by mutation of

further arginines (Fig. 6). These results are in agreement with those reporting the main

participation of positively charged amino acids in RNA binding activity of diverse viral

proteins (Ansel-McKinney et al., 1996; Genovés et al., 2009; Herranz and Pallás, 2004;

1   Martínez-Turiño and Hernández, 2010; Rao and Grantham, 1996; Wobbe et al., 1998).

2   In addition, the *in vitro* studies have revealed that PFBV p12, as other MPs (Brill et al.,

3   2000; Herranz and Pallás, 2004; Navarro et al., 2006), has a preference for single-

4   stranded nucleic acids, particularly to ssRNA that apparently binds in a sequence non-

5   specific manner. Sequence specificity *in vivo* is likely afforded through other viral-

6   and/or host-coded proteins. Alternatively, compartimentalization of viral components

7   could preclude the protein from association to and movement of cellular RNAs. It is

8   also noteworthy that, according the estimated K_d (3.14 μM), the affinity of p12 for

9   ssRNA is similar to that determined for carmoviral DGBps1 like CarMV p7 and MNSV

10   p7A (1.1 μM and 25.7 μM, respectively; Marcos et al., 1999; Navarro et al., 2006),

11   suggesting that this p12 activity is not marginal or secondary but relevant during the

12   infectious process.

13   To conclude, we have proven the requirement of the leucine zipper-like motif and of

14   the N-terminal extension of PFBV p12 for effective viral infection. We do not know at

15   this stage which particular conditions have driven the evolution of such specific traits.

16   We can speculate that the answer to this issue is related with the adaptation of the virus

17   to its narrow host range as PFBV is restricted to *Pelargonium* spp. in nature. Significant

18   examples of carmovirus adaptation, including PFBV, to a particular host have been

19   described (Liang et al., 2002a; Rico et al., 2006). Remarkable in this context is the

20   finding that *Hibiscus chlorotic ringspot viru*s encodes a protein (p23) that has no

21   homologs in other carmoviruses and that confers host specificity. Curiously, such a

22   protein, as PFBV p12, contains a putative leucine zipper though the biological

23   significance of the motif has yet to be explored (Liang et al., 2002b). On the other hand,

24   the present study raises new questions on the role(s) of the DGBp partners during virus

25   movement. As mentioned in the Introduction section, recent results suggest that MNSV

1 DGBp1 cannot only bind the viral genome but probably has also the capacity to

2 transport it toward PD following a route different from that used by MNSV DGBp2

3 (Genovés et al., 2009, 2010). The role of the latter protein would then be uncertain but it

4 could be related with PD gating rather than with the intracellular movement of the

5 DGBp1-genome complex as initially proposed. In the case of PFBV, the RNA binding

6 ability of DGBp2 and, most likely, of DGBp1 could provide an additional advantage to

7 the virus by potentially increasing the number of viral genomes that can reach and pass

8 through the intercellular connections, thus facilitating the spread of the pathogen.

9 Additional work might provide further clues on this attracting possibility.

10 **Materials and methods**

11 *Generation of constructs*

12 Site-directed mutations affecting ORFs p7 and p12 were introduced into the PFBV

13 infectious clone pSP18-IC (Rico and Hernández, 2006) by PCR using with the Quick

14 Change Site-Directed Mutagenesis kit (Stratagene) and proper oligonucleotide pairs.

15 The mutations altered the presumed start codons of each ORF or led to amino acid

16 replacements in selected regions of p12.

17 Binary constructs for transient expression in plants were generated as follows. ORF

18 p12 was PCR amplified from the infectious clone pSP18-IC using specific primer pairs

19 and the Expand High Fidelity PCR System (Roche). The amplification product, bearing

20 proper restriction sites at the ends, was fused in frame to the 5´ end of the GFP or

21 monomeric (m) RFP genes by standard cloning procedures (Sambrook et al., 2007). The

22 unfused GFP gene and the DNA fusions p12GFP and p12mRFP were inserted between

23 the *Cauliflower mosaic virus* (CaMV) 35S promoter and the terminator sequence of the

24 *Solanum tuberosum* proteinase inhibitor II gene (PoPit) and cloned into the binary

1 vector pMOG800 (Knoester et al., 1998) to yield constructs pMOG-GFP, pMOG-

2 p12GFP and pMOG-p12mRFP, respectively.

3   A similar approach was followed to obtain constructs for protein expression in *E.*

4 *coli*. Full-length and truncated forms of ORF p12 were PCR amplified and cloned into

5 the pET-23d(+) vector (Novagen) through its *Nco*I and *Hind*III restriction sites. The

6 resulting recombinant plasmids, named pET-p12, pET-p12(1-59) and pET-p12(26-106),

7 contained the corresponding version of the PFBV gene fused to a sequence coding for a

8 hexa-histidine tag. Three additional constructs, pET-p12(1-59)mut2R, pET-p12(1-

9 59)mut3R and pET-p12(1-59)mut4R, identical to pET-p12(1-59) but with nucleotide

10 substitutions that led to the replacement of two, three and four arginine residues by

11 alanines, respectively, in the corresponding proteins were generated by PCR with the

12 Quick Change Site-Directed Mutagenesis kit (Stratagene). All constructs were routinely

13 sequenced with an ABI PRISM DNA sequencer 377 (Perkin-Elmer) to avoid unwanted

14 modifications. The primers used to generate the distinct plasmids are listed in Table 1.

15 Representation of the type and specific position of the modifications introduced in each

16 mutant construct is shown in the corresponding figures.

17 *Inoculation of plants and protoplasts*

18   Transcripts were synthesized *in vitro* from wt clone pSP18-IC and derived mutant

19 constructs with T7 RNA polymerase (Fermentas) following digestion of plasmids with

20 *Xba*I. Protoplasts (0.5×10^6), prepared from *C. quinoa* leaves (Hans et al., 1992), were

21 inoculated with 10 µg of PFBV genomic transcripts by using polyethylene glycol. The

22 same type of transcripts was used to mechanically inoculate *C. quinoa* plants (three

23 leaves per plant employing approximately 2 µg of transcript per leave). Plants were

1 maintained under greenhouse conditions (16 h days at 24 ºC, 8 h nights at 20 ºC) and

2 monitored for lesion appearance from 7 to 15 dpi.

3 *RNA extraction and Northern blot hybridization*

4   Total RNA preparations from *C. quinoa* leaves were obtained by phenol extraction

5 and lithium precipitation (Verwoerd et al., 1989). In addition, total RNA was extracted

6 from protoplast samples using TRI Reagent according the manufacturers instructions

7 (SIGMA). Northern blot analysis was performed with a ^{32}P-radioactive DNA probe,

8 derived from the 3´ region of PFBV genome, as previously described (Rico and

9 Hernández, 2009).

10 *Agrobacterium-mediated transient expression, subcellular fractionation and*

11 *immunoblotting*

12   For transient expression in plants, constructs pMOG-GFP, pMOG-p12GFP and

13 pMOG-p12mRFP were used to transform *Agrobacterium tumefaciens* strain C58C1

14 (pCH32). Transformed bacteria were grown overnight in proper conditions and

15 subsequently collected by slow-speed centrifugation and adjusted to the required final

16 OD_{600} (0.5) value with 10 mM $MgCl_2$, 10 mM MES, pH 5.6 and 150 µM

17 acetosyringone. After 2 h incubation, the suspensions were infiltrated with a 5 ml

18 needleless syringe on the abaxial side of leaves from 3-week-old *N. benthamiana* plants

19 as previously described (Martínez-Turiño and Hernández, 2009).

20   To prepare soluble and insoluble fractions from GFP and p12GFP-expressing plant

21 tissue, *N. benthamiana* leaves were collected 5 days after agroinfiltration with the

22 corresponding construct and ground with a mortar and pestle with 5 ml of extraction

23 buffer (50 mM Tris-acetate, pH 7.4, 10 mM potassium acetate, 1 mM EDTA, 5 mM

24 dithiothreitol, 0.5 mM phenylmethylsulfonyl fluoride) per g of fresh weight. After

1 extraction, the homogenates were centrifuged at 3,000 × *g* for 10 min to remove large

2 cellular debris and the resulting supernadant was ultracentrifuged at 30,000 × *g* for 1 h

3 to generate the soluble (S30) and the microsomal (P30) fractions. Then, the P30 fraction

4 was resuspended in 500 μl of extraction buffer. The S30 and P30 fractions were

5 electrophoresed, transferred to polyvinylidene fluoride membranes (PVDF) membranes

6 (Roche) and immunoblotted with anti-GFP (Roche). Immunoreactive bands were

7 revealed with chemiluminescence ECL Plus kit following supplier recommendations

8 (GE Healthcare).

9 *Fluorescence microscopy*

10   A Leica TCS SL confocal microscope was used to obtain images employing an

11 HCX PL APO ×40/1.25-0.75 oil CS objective. GFP fluorescence was monitored by

12 excitation with 488 nm argon laser line with emission being collected through band-

13 pass filter from 505 to 550 nm. In the case of mRFP, excitation was performed by

14 means of a 543-nm green-neon laser line, and fluorescence emission was collected at

15 610 to 630 nm. Observation of fluorescence in agroinfiltrated *N. benthamiana* leaves

16 was done at 48-72 h post-infiltration.

17 *Expression and purification of PFBV p12 and derivatives*

18   The pET-23d(+)-based constructs were used to transform *E. coli* Rosetta

19 (DE3)pLysS (Novagen). Expression of the His-tagged p12 protein and derivatives was

20 induced in the transformed bacteria with isopropyl-b-D-thiogalactopiranoside (IPTG) at

21 0.4 mM for 4 h at 37 ºC. Purification of the proteins was performed by metal affinity

22 chromatography in denaturing conditions using nickel-nitrilotriacetic acid (Ni-NTA)

23 columns and following manufacturer recommendations (Sigma). His-tagged proteins

24 were finally eluted from the columns in a buffer containing 500 mM imidazole, 300

mM NaCl and 50mM NaH_2PO_4/Na_2HPO_4, pH 8.0. Purified preparations were dialysed at 4 ºC for 24 h against PBS 1x (136 mM NaCl, 2.7 mM KCl, 3.2 mM Na_2HPO_4, 1.5 mM KH_2PO_4, pH 7.5) supplemented with Arg and Glu at 50 mM in order to favour the stability of the proteins (Golovanov et al., 2004). The purified recombinant proteins were analyzed and quantified by SDS-15 % PAGE after Coomassie brilliant blue staining.

EMSA

A ^{32}P-labeled ssRNA probe named 5´-PFBV and embracing the 5´-terminal 141 nt of PFBV genome was used for EMSA. The ^{32}P-labeled RNA probe (at 97 pM) was mixed with p12 and derivatives at different ratios in 25 μl of binding buffer (50 mM Tris-HCl, pH 8.0, 50 mM NaCl, 0.1 mM EDTA, 10 % glycerol and 2 U of RNase inhibitor [Fermentas]) and incubated at 25 ºC for 30 min. When indicated, the NaCl concentration was modified. After the binding reaction, samples were analyzed by non-denaturing PAGE (5%) in TAE buffer (40 mM Tris-HCl, 20 mM sodium acetate, 1mM EDTA, pH 7.2). The gel was vacuum dried and exposed for autoradiography or phosphorimage analysis. In competition experiments, different amounts of unlabeled nucleic acids were added simultaneously with the labeled ssRNA probe to the binding mixtures. Competitors corresponded to two distinct ssRNAs, namely 3´-PFBV (encompassing nt 3560-3923 of the PFBV genome) and het-ssRNA (non-PFBV ssRNA), and to heterologous dsRNA, ssDNA and dsDNA molecules. Synthesis of the labelled probe and of the different competitors was performed as previously described (Martínez-Turiño and Hernández, 2010). GraphPad Prism software version 5.03 was employed for non-linear regression analysis of the binding data and for estimation of K_d and IC_{50} values.

1 *Northwestern assay*

2   Recombinant proteins pET-p12(1-59), pET-p12(26-106), pET-p12(1-59)mut2R,

3 pET-p12(1-59)mut3R and pET-p12(1-59)mut4R were electrophoresed through 15%

4 SDS-polyacrylamide gels and electroblotted to nitrocellulose membranes (Scheicher

5 and Schuell) in the presence of transfer buffer (25 mM Tris, 192 mM glycine and 20%

6 methanol). The membrane attached proteins were renatured overnight at room

7 temperature in renaturation buffer (10 mM Tris– HCl pH 7.5, 1 mM EDTA, 50 mM

8 NaCl, 0.1% Triton X-100 and $1\times$ Denhardt's reagent) supplemented with 1 % BSA. The

9 membranes were then probed with ^{32}P- labelled 3´-PFBV ssRNA, washed three times

10 with the renaturation buffer, air dried and subjected to autoradiography.

11 *Sequence analyses*

12   A consensus secondary structure of PFBV p12 was drawn from data obtained by

13 means of SYMPRED server (http://www.ibi.vu.nl/programs/sympredwww/) (Simossis

14 and Heringa, 2004), that was run using a combination of different programs (JNet,

15 PSIPred PHDpsi, SSPro2.01, YASPIN and PREDATOR). Hydrophobic regions with

16 potential membrane insertion were determined through programs SOUSI, TMPRED,

17 DAS, TMHMM2 HMMTop 2.0 and TopPred2 available at the Expasy Proteomics

18 server (http://expasy.org/tools/#proteome) (Gasteier et al., 2003). Softwares NetPhos

19 2.0 and YinOYang 1.2 were used from the same server for prediction of potential

20 phosphorylation and glycosylation sites in the protein.

21 **Acknowledgements**

References

Ansel-McKinney, P., Scott, S.W., Swanson, M., Ge, X., Gehrke, L., 1996. A plant viral coat protein RNA binding consensus sequence contains a crucial arginine. EMBO J. 15, 5077-5084.

Akgoz, M., Nguyen, Q.N., Talmadge, A.E., Drainville, K.E., Wobbe, K.K., 2001, Mutational analysis of *Turnip crinkle virus* movement protein p8. Mol. Plant Pathol. 2, 37-48.

Benitez-Alfonso, Y., Faulkner, C., Ritzenthaler, C., Maule, A., 2010. Plasmodesmata: gateways to local and systemic virus infection. Mol. Plant Microbe Interact. 23, 1403-1412.

Bornberg-Bauer, E., Rivals, E., Vingron, M., 1998. Computational approaches to identify leucine zippers. Nucleic Acids Res. 26, 2740–2746.

Brantley, J.D., Hunt, A.G., 1993. The N-terminal protein of the polyprotein encoded by the potyvirus *Tobacco vein mottling virus* is an RNA-binding protein. J. Gen. Virol. 74, 1157-1162.

Brill, L.M., Nunn, R.S., Kahn, T.W., Yeager, M., Beachy, R.N., 2000. Recombinant *Tobacco mosaic virus* movement protein is an RNA-binding, alpha-helical membrane protein. Proc. Natl. Acad. Sci. U.S.A. 97, 7112-7117.

1   Busch, S.J., Sassone-Corsi, P., 1990. Dimers, leucine zippers and DNA-binding

2   domains. Trends Genet. 6, 36-40.

3   Chen, Y., Varani, G., 2005. Protein families and RNA recognition. FEBS J. 272, 2088–

4   2097.

5   Chevalier, F., Perazza, D., Laporte, F., Le Hénanff, G., Hornitschek, P., Bonneville,

6   J.M., Herzog, M., Vachon, G., 2008. GeBP and GeBP-like proteins are

7   noncanonical leucine-zipper transcription factors that regulate cytokinin response in

8   *Arabidopsis*. Plant Physiol. 146, 1142-1154.

9   Citovsky, V., Knorr, D., Schuster, G., Zambryski, P., 1990. The P30 movement protein

10   of *Tobacco mosaic virus* is a single strand nucleic acid binding protein. Cell 60,

11   637–647.

12   Daròs, J.A., Carrington, J.C., 1997. RNA binding activity of NIa proteinase of *Tobacco*

13   *etch potyvirus*. Virology 237, 327–336.

14   Desvoyes, B., Faure-Rabasse, S., Chen, M.H., Park, J.W., Scholthof, H.B., 2002. A

15   novel plant homeodomain protein interacts in a functionally relevant manner with a

16   virus movement protein. Plant Physiol. 129, 1521-1532.

17   Fetchko, M., Stagljar, I., 2004. Application of the split-ubiquitin membrane yeast two-

18   hybrid system to investigate membrane protein interactions. Methods 32, 349-362.

19   Fry, A.M., Arnaud, L., Nigg, E.A., 1999. Activity of the human centrosomal kinase,

20   Nek2, depends on an unusual leucine zipper dimerization motif. J. Biol. Chem. 274,

21   16304-16310.

1   Gasteiger, E., Gattiker, A., Hoogland, C., Ivanyi, I., Appel, R.D., Bairoch, A., 2003.

2   ExPASy: The proteomics server for in-depth protein knowledge and analysis.

3   Nucleic Acids Res. 31, 3784-3788.

4   Genovés, A., Navarro, J.A., Pallás, V., 2006. Functional analysis of the five *Melon*

5   *necrotic spot virus* genome-encoded proteins. J. Gen. Virol. 87, 2371-2380.

6   Genovés, A, Navarro, J.A., Pallás V., 2009. A self-interacting carmovirus movement

7   protein plays a role in binding of viral RNA during the cell-to-cell movement and

8   shows an actin cytoskeleton dependent location in cell periphery. Virology 395,

9   133-142.

10 Genovés, A, Navarro, J.A., Pallás, V., 2010. The intra- and intercellular movement of

11   *Melon necrotic spot virus* (MNSV) depends on an active secretory pathway. Mol.

12   Plant Microbe Interact. 23, 263-272.

13 Golovanov, A.P., Hautbergue, G.M., Wilson, S.A., Lian, L.Y., 2004. A simple method

14   for improving protein solubility and long-term stability. J. Am. Chem. Soc. 126,

15   8933-8939.

16 Hacker, D.L., Petty, I.T., Wei, N, Morris, T.J., 1992. *Turnip crinkle virus* genes

17   required for RNA replication and virus movement. Virology 186, 1-8.

18 Hans, F., Fuchs, M., Pinck, L., 1992. Replication of *Grapevine fanleaf virus* satellite

19   RNA transcripts in *Chenopodium quinoa* protoplasts. J. Gen. Virol. 73, 2517-2523.

20 Harries, P.A., Schoelz, J.E., Nelson, R.S., 2010. Intracellular transport of viruses and

21   their components: utilizing the cytoskeleton and membrane highways. Mol. Plant

22   Microbe Interact. 23, 1381-1393.

1   Haupt, S., Cowan, G.H., Ziegler, A, Roberts, A.G., Oparka, K.J., Torrance, L., 2005.

2   Two plant-viral movement proteins traffic in the endocytic recycling pathway. Plant

3   Cell 17, 164-181.

4   Heinlein, M., Epel, B.L., 2004. Macromolecular transport and signaling through

5   plasmodesmata. Int. Rev. Cytol. 235, 93–164.

6   Heinlein, M., Padgett, H.S., Gens, J.S., Pickard, B.G., Casper, S.J., Epel, B.L, Beachy,

7   R.N., 1998. Changing patterns of localization of the *Tobacco mosaic virus*

8   movement protein and replicase to the endoplasmic reticulum and microtubules

9   during infection. Plant Cell 10, 1107–1120.

10   Herranz, M.C., Pallás, V., 2004. RNA-binding properties and mapping of the RNA-

11   binding domain from the movement protein of *Prunus necrotic ringspot virus*. J.

12   Gen. Virol. 85, 761–768.

13   Hull, R., 2002. Virus movement through the plant and effects on plant metabolism,

14   Matthews' plant virology, 4th Ed. Academic Press, San Diego, pp. 373–436.

15   Ju, H.J., Samuels, T.D., Wang, Y.S., Blancaflor, E., Payton, M., Mitra, R.,

16   Krishnamurthy, K., Nelson, R.S., Verchot-Lubicz, J., 2005. The *Potato virus X*

17   TGBp2 movement protein associates with endoplasmic reticulum-derived vesicles

18   during virus infection. Plant Physiol. 138, 1877-1895.

19   Kawakami, S., Hori K., Hosokawa, D., Okada, Y., Watanabe, Y., 2003. Defective

20   tobamovirus movement protein lacking wild-type phosphorylation sites can be

21   complemented by substitutions found in revertants. J. Virol. 77, 1452-1461.

1 Knoester, M., van Loon, L.C., van den Heuvel, J., Hennig, J., Bol, J.F., Linthorst,
2 H.J.M., 1998. Ethylene-insensitive tobacco lacks nonhost resistance against soil-
3 borne fungi. Proc. Natl. Acad. Sci. U.S.A. 95, 1933–1937.

4 Landschulz, W.H., Johnson, P.F., McKnight, S.L., 1998. The leucine zipper: a
5 hypothetical structure common to a new class of DNA binding proteins. Science
6 240, 1759–1764.

7 Leh, V., Jacquot, E., Geldreich, A., Haas, M., Blanc, S., Keller, M., Yot, P., 2001.
8 Interaction between the open reading frame III product and the coat protein is
9 required for transmission of *Cauliflower mosaic viru*s by aphids. J. Virol. 75, 100-
10 106.

11 Li, W.Z., Qu, F., Morris, T.J., 1998. Cell-to-cell movement of *Turnip crinkle virus* is
12 controlled by two small open reading frames that function *in trans.* Virology 244,
13 405–416.

14 Liang, X.Z., Lee, B.T.K., Wong, S.M. 2002a. Covariation in the capsid protein of
15 *Hibiscus chlorotic ringspot virus* induced by serial passaging in a host that restricts
16 movement leads to avirulence in its systemic host. J. Virol. 76, 12320-12324.

17 Liang, X.Z., Lucy, A.P., Ding, S.W., Wong, S.M., 2002b. The p23 protein of *Hibiscus*
18 *chloritc ringspot virus* is indispensable for host-specific replication. J. Virol. 76,
19 12312-12319.

20 Lommel, S.A., Martelli, G.P., Rubino, L., Russo, M., 2005. Family *Tombusviridae,* in:
21 Fauquet, C.M., Mayo, M.A., Maniloff, J., Desselberger, U., Ball, L.A. (Eds.), Eighth
22 Report of the International Committee on Taxonomy of Viruses. Academic Press,
23 San Diego, USA, pp. 907-936.

1   Long, G., Pan, X., Vlak, J.M., 2008. Conserved leucines in N-terminal heptad repeat

2   HR1 of envelope fusion protein F of group II nucleopolyhedroviruses are important

3   for correct processing and essential for fusogenicity. J. Virol. 82, 2437-2447.

4   López, C., Navas-Castillo, J., Gowda, S., Moreno, P., Flores, R., 2000. The 23-kDa

5   protein coded by the 3′-terminal gene of *Citrus tristeza virus* is an RNA-binding

6   protein. Virology 269, 462-470.

7   Luan, C.H., Qiu, S., Finley, J.B., Carson, M., Gray, R.J., Huang, W., Johnson., D.,

8   Tsao, J., Reboul, J., Vaglio, P., Hill, D.E., Vidal, M., Delucas, L.J., Luo, M., 2004.

9   High-throughput expression of *C. elegans* proteins. Genome Res. 14, 2102-2110.

10   Lucas, W.J., 2006. Plant viral movement proteins: agents for cell-to-cell trafficking of

11   viral genomes. Virology 344, 169–184.

12   Lyu, P.C., Liff, M.I., Marky, L.A., Kallenbach, N.R., 1990. Side chain contributions to

13   the stability of alpha-helical structure in peptides. Science 250, 669–673.

14   Marcos, J.F., Vilar, M., Pérez-Payá, E., Pallás, V., 1999. *In vivo* detection, RNA-

15   binding properties and characterization of the RNA-binding domain of the p7

16   putative movement protein from carnation mottle carmovirus (CarMV). Virology

17   255, 354–365.

18   Martínez-Gil, L., Johnson, A.E., Mingarro, I., 2010. Membrane insertion and biogenesis

19   of the *Turnip crinkle virus* p9 movement protein. J. Virol. 84, 5520-5527.

20   Martínez-Turiño, S., Hernández, C., 2009. Inhibition of RNA silencing by the coat

21   protein of *Pelargonium flower break virus*: distinctions from closely related

22   suppressors. J. Gen. Virol. 90, 519-525.

1   Martínez-Turiño, S., Hernández, C., 2010. Identification and characterization of RNA

2   binding activity in the ORF1-encoded replicase protein of *Pelargonium flower break*

3   *virus*. J. Gen. Virol. 91, 3075-3084.

4   Melcher, U., 2000. The '30K' superfamily of viral movement proteins. J. Gen. Virol.

5   81, 257–266.

6   Moitra, J., Szilák, L., Krylov, D., Vinson, C., 1997. Leucine is the most stabilizing

7   aliphatic amino acid in the d position of a dimeric leucine zipper coiled coil.

8   Biochemistry 36, 12567-12573.

9   Navarro, J.A., Genovés, A., Climent, J., Saurí, A., Martínez-Gil, L., Mingarro, I., Pallás,

10   V., 2006. RNA-binding properties and membrane insertion of *Melon necrotic spot*

11   *virus* (MNSV) double gene block movement proteins. Virology 356, 57-67.

12   Nelson, R.S., Citovsky, V., 2005. Plant viruses. Invaders of cells and pirates of cellular

13   pathways. Plant Physiol. 138, 1809–1814.

14   O'Neil, K.T., DeGrado, W.F., 1990. A thermodynamic scale for the helix-forming

15   tendencies of the commonly occurring amino acids. Science 250, 646–651.

16   O'Shea, E.K., Rutkowski, R., Kim, P.S., 1989. Evidence that the leucine zipper is a

17   coiled coil. Science 243, 538–542.

18   Pagano, M., Clynes, M.A., Masada, N., Ciruela, A., Ayling, L.J., Wachten, S., Cooper,

19   D.M., 2009. Insights into the residence in lipid rafts of adenylyl cyclase AC8 and its

20   regulation by capacitative calcium entry. Am. J. Physiol. Cell Physiol. 296, C607-

21   619.

1   Peremyslov, V.V., Pan, Y.W., Dolja, V.V., 2004. Movement protein of a closterovirus

2   is a type III integral transmembrane protein localized to the endoplasmic reticulum.

3   J. Virol. 78, 3704-3709.

4   Rao, A.L., Grantham, G.L., 1996. Molecular studies on bromovirus capsid protein. II.

5   Functional analysis of the amino-terminal arginine-rich motif and its role in

6   encapsidation, movement, and pathology. Virology 226, 294-305.

7   Richmond, K.E., Chenault, K., Sherwood, J.L., German, T.L., 1998. Characterization of

8   the nucleic acid binding properties of *Tomato spotted wilt virus* nucleocapsid

9   protein. Virology 248, 6–11.

10   Rico, P., Hernández, C., 2004. Complete nucleotide sequence and genome organization

11   of *Pelargonium flower break virus*. Arch. Virol. 149, 641-651.

12   Rico, P., Hernández, C., 2006. Infectivity of *in vitro* transcripts from a full length cDNA

13   clone of *Pelargonium flower break virus* in an experimental and a natural host. J.

14   Plant Pathol. 88, 103-106.

15   Rico, P., Hernández, C., 2009. Characterization of the subgenomic RNAs produced by

16   *Pelargonium flower break virus*: identification of two novel RNA species. Virus

17   Res. 142, 100-107.

18   Rico, P., Ivars, P., Elena, S.F., Hernández, C., 2006. Insights on the selective pressures

19   restricting *Pelargonium flower break virus* genome variability: evidence for host

20   adaptation. J. Virol. 80, 8124-8132.

21   Ruiz, M.T., Voinnet, O., Baulcombe, D.C., 1998. Initiation and maintenance of virus-

22   induced gene silencing. Plant Cell 10, 937-946.

1   Sambrook, J., Fritsch, E.F., Maniatis, T., 2007. Molecular Cloning: A Laboratory

2   Manual. Cold Spring Harbor Laboratory Press, Cold Spring Harbor, N.Y., U.S.A.

3   Saurí, A., Saksena, S., Salgado, J., Johnson, A.E., Mingarro, I., 2005. Double-spanning

4   plant viral movement protein integration into the endoplasmic reticulum membrane

5   is signal recognition particle-dependent, translocon-mediated, and concerted. J. Biol.

6   Chem. 280, 25907-25912.

7   Skuzeski, J.M., Morris, T.J., 1995. Quantitative analysis of the binding of *Turnip*

8   *crinkle virus* coat protein to RNA fails to demonstrate binding specificity but reveals

9   a highly cooperative assembly interaction. Virology 210, 82–90.

10   Schepetilnikov, M.V., Solovyev, A.G., Gorshkova, E.N., Schiemann, J., Prokhnevsky,

11   A.I., Dolja, V.V., Morozov, S.Y., 2008. Intracellular targeting of a hordeiviral

12   membrane-spanning movement protein: sequence requirements and involvement of

13   an unconventional mechanism. J. Virol. 82, 1284-1293.

14   Simossis, V.A, Heringa, J., 2004. Optimally segmented consensus secondary structure

15   prediction. SYMPRED server at URL: http://ibivu.cs.vu.nl/programs/

16   sympredwww/.

17   Takemoto, Y., Hibi, T., 2005. Self-interaction of ORF II protein through the leucine

18   zipper is essential for *Soybean chlorotic mottle virus* infectivity. Virology 332, 199-

19   205.

20   Takemoto, Y., Kanehira, T., Shinohara, M., Yamashita, S., Hibi, T., 2000. The

21   nucleotide sequence and genome organization of *Japanese iris necrotic ring virus*, a

22   new species in the genus *Carmovirus*. Arch. Virol. 145, 651-657.

1   Verwoerd, T.C., Dekker, B.M.M., Hoekema, A., 1989. A small-scale procedure for the
2   rapid isolation of plant RNAs. Nucleic Acids Res. 17, 2362.

3   Vilar, M., Esteve, V., Pallás, V., Marcos, J.F, Pérez-Payá, E., 2001. Structural
4   properties of *Carnation mottle virus* p7 movement protein and its RNA-binding
5   domain. J. Biol. Chem. 276, 18122–18129.

6   Vilar, M., Saurí, A., Monné, M., Marcos, J.F., von Heijne, G., Pérez-Payá, E.,
7   Mingarro, I., 2002. Insertion and topology of a plant viral movement protein in the
8   endoplasmic reticulum membrane. J. Biol. Chem. 277, 23447-23452.

9   Vilar, M., Saurí, A., Marcos, J.F., Mingarro, I., Pérez-Payá, E., 2005. Transient
10   structural ordering of the RNA-binding domain of *Carnation mottle virus* p7
11   movement protein modulates nucleic acid binding. Chembiochem. 6, 1391-1396.

12   Waigmann, E., Ueki, S., Trutnyeva, K., Citovsky, V., 2004. The ins and outs of non-
13   destructive cell-to-cell and systemic movement of plant viruses. Crit. Rev. Plant Sci.
14   23, 195–250.

15   Weiss, M.A., Narayana, N., 1998. RNA recognition by arginine-rich peptide motifs.
16   Biopolymers 48, 167–180.

17   Wobbe, K.K., Akgoz, M., Dempsey, D.A., Klessig, D.F., 1998. A single amino acid
18   change in *Turnip crinkle virus* movement protein p8 affects RNA binding and
19   virulence on *Arabidopsis thaliana.* J. Virol. 72, 6247–6250.

20   Zhang, X.J., Baase, W.A., Matthews, B.W., 1991. Toward a simplification of the
21   protein folding problem: a stabilizing polyalanine alpha-helix engineered in T4
22   lysozyme. Biochemistry 30**,** 2012–2017.

1 **LEGENDS TO FIGURES**

2 **Fig. 1.** Bioassay of PFBV mutants. (A) Schematic representation of wt PFBV gRNA

3 (top) and derived mutants p7aug- and p12aug- (bottom). Nucleotide positions of the

4 initiation codons of ORFs p7 and p12 are indicated. Substitutions affecting these codons

5 were introduced into the full-length cDNA clone pSP18-IC leading to triplet changes

6 that are depicted for each mutant. The engineered mutations did not alter the amino acid

7 sequences of overlapping ORFs. In mutants, dashed boxes correspond to ORFs that are

8 not expected to be translated. (B) Northern blot hybridization of total RNA extracted

9 from *C. quinoa* leaves (left panel) or protoplasts (right panel) inoculated with transcripts

10 corresponding to the PFBV wt construct (lane 1) or to mutants p7aug- and p12aug-

11 (lanes 2 and 3, respectively). Lanes 0 correspond to mock-inoculated negative controls.

12 The arrow marks the position of the gRNA; lower bands correspond to subgenomic

13 RNAs. Ethidium bromide staining of rRNA was used as a loading control.

14

15 **Fig. 2.** Effect of amino acid substitutions in the leucine zipper-like domain of p12 on

16 virus infection. (A) *Top*. Schematic diagram of p12 showing the relative location of the

17 putative leucine zipper motif (LZ) in relation to other predicted domains of the protein.

18 Boundaries of each domain are indicated. BRD: domain at the N-terminus rich in basic

19 amino acids; TM: stretch of residues predicted to be involved in α-helix or

20 transmembrane segments; LZ: leucine zipper-like domain; BS: β-sheet structured

21 region. *Bottom*. Aminoacid sequence of the leucine zipper-like motif in wt and mutant

22 constructs. Dashed lines represent residues identical to the wt protein whereas specific

23 amino acid replacements are indicated for each mutant. The seven positions of the

24 heptad repeat are labeled "a" through "g". The residues found at critical "d" positions

are highlighted in boldface type. (B) Northern blot hybridization of total RNA extracted from plants (left panel) or protoplasts (right panel) inoculated with transcripts corresponding to the PFBV wt construct (lane 1) or mutants LZM1 to LZM6 (lanes 2 to 7) as indicated above the lanes. Lanes 0 correspond to buffer-inoculated negative controls. The arrow marks the position of the genomic RNA; lower bands correspond to subgenomic RNAs. Ethidium bromide staining of rRNA was used as a loading control.

Fig. 3. Studies on the subcellular localization of PFBV p12 in *N. benthamiana* leaves through transient expression. (A to C) Confocal scanning microscopy analysis of non-transgenic *N. benthamiana* leaves expressing unfused GFP (A, green channel) or the p12GFP fusion (B and C, green channel). (D to F) Confocal scanning microscopy analysis of leaves from transgenic 16c *N. benthamiana* plants expressing an ER-targeted GFP (Ruiz et al., 1998), after agroinfiltration with the construct that allows translation of the p12mRFP fusion. D and E display images through the red and green channel, respectively, and F corresponds to an overlay. (G) Immunoblot analysis, using anti-GFP antibody, of protein extracts from GFP- and p12GFP- expressing *N. benthamiana* leaves (right and left blots, respectively). S30 (lane 1) and P30 (lane 2), supernatant and pellet, respectively, following centrifugation at 30,000 x *g*.

Fig. 4. Analysis of RNA-binding properties of PFBV p12 *in vitro*. (A) Representative EMSA showing interactions between the recombinant p12 and ssRNA. The ^{32}P-labeled 5′-PFBV ssRNA probe (at 97 pM) was incubated with no protein (lane 1) or with His-tagged p12 at 0.10, 0.21, 0.33, 3.70, 6.55, 13.10, 26.20 and 52.41 μM (lanes 2 to 9, respectively). The unbound, free RNA probe and the shifted (bound) RNA complexes

are marked on the right. (B) Best-fit curve of the binding data from three independent experiments determined by non-linear regression. (C) Effect of NaCl concentration on the RNA binding activity of PFBV p12. The fraction of bound ssRNA was plotted against the log[NaCl] (in mM) to estimate the IC_{50} value.

Fig. 5. Competition assays to evaluate binding specificity of p12. (A) EMSAs performed after incubation of His-tagged p12 (32.75 μM) and ^{32}P-labeled, 5′-PFBV ssRNA probe (at 97.0 pM) in the absence (lane 2) or the presence (lanes 3 to 17) of increasing amounts (1, 10- and 100-fold molar excess) of unlabeled competitors as shown at the top of the autoradiograms. Lanes 1, no protein. (B) Graphical representation of the EMSA results. The percentage of free probe has been plotted against competitor/probe molar ratio. The experiments were repeated twice with essentially identical results (data of one set of experiments are presented here).

Fig. 6. Mapping the RNA binding domain of p12. (A) Schematic representation of p12 and its mutant forms, p12(26-106), p12(1-59), p12(1-59)m2R, p12(1-59)m3R, p12(1-59)m4R. Dashed lines indicate deleted regions in the truncated forms. In mutant versions, replacement of arginine residues by alanines are indicated. (B) Northwestern analysis of p12 and mutated forms. The purified recombinant proteins were separated by SDS-15% PAGE as shown in the left panel after Coomasie blue staining, and transferred to a nitrocellulose membrane that was incubated with the ^{32}P-labeled ssRNA probe (5′-PFBV) and autoradiographed as shown in the right panel. The asterisk in the left panel marks the position of a non-specific protein band.

Table 1. List of primers used in this work

Primer	Positionᵃ	Sequenceᵇ		Construct
CH349	2276-2303 (S)	5´ CCACACAATTGAgTGGCTTCTAAAGTGA-3´		p7aug-
CH350	2276-2303 (AS)	5´-TCACTTTAGAAGCCAcTCAATTGTGTGG-3´		
CH79	2317-2342 (S)	5´-GGGTAGTGATAAcGAGATTGACGTGC-3´		p12aug-
CH80	2317-2342 (AS)	5´-GCACGTCAATCTCgTTATCACTACCC-3´		
CH81	2516-2540 (S)	5´-CCAACACATAaTcAATCTTACCTTG-3´		LZM1
CH82	2516-2540 (AS)	5´-CAAGGTAAGATTgAtTATGTGTTGG-3´		LZM5
CH83	2514-2537 (S)	5´-CTCCAACACATAgcGAATCTTACC-3´		LZM2
CH84	2514-2537 (AS)	5´-GGTAAGATTCgcTATGTGTTGGAG-3´		LZM6
CH85	2557-2580 (S)	5´-GTTCTTTCATCcgGGCAGAGAGAG-3´		LZM3
CH86	2557-2580 (AS)	5´-CTCTCTCTGCCcgGATGAAAGAAC-3´		LZM5
CH87	2557-2580 (S)	5´-GTTCTTTCATCgcGGCAGAGAGAG-3´		LZM4
CH88	2557-2580 (AS)	5´-CTCTCTCTGCCgcGATGAAAGAAC-3´		LZM6
CH39	2328-2347 (S)	5´-GGGGGATCCATGAGATTGACGTGTCAGTG-3´	(*Bam*HI)	pMOG-p12GFP
CH38	2626-2645 (AS)	5´-GGAAGCTTAGGATCCTTGCCCAGTTGAGATCCGTA-3´	(*Bam*HI)	pMOG-p12mRFP
DH5P12	2328-2351 (S)	5´-GGCCATGGGATTGACGTGTCAGTGGGAG-3´	(*Nco*I)	pET-p12
CH69	2625-2645 (AS)	5´-CCAAGCTTTTGCCCAGTTGAGATCCGTAT-3´	(*Hind*III)	
DH5P12	2328-2351 (S)	5´-GGCCATGGGATTGACGTGTCAGTGGGAG-3´	(*Nco*I)	pET-p12(1-59)
CH96	2482-2504 (AS)	5´-CCAAGCTTAGGGGGCATACTAAAAGTTGAAG-3´	(*Hind*III)	
CH265	2401-2423 (S)	5´-GGCCATGGCGCTGTCTCCAAACGGACATCTG-3´	(*Nco*I)	pET-p12(26-106)
CH69	2625-2645 (AS)	5´-CCAAGCTTTTGCCCAGTTGAGATCCGTAT-3´	(*Hind*III)	
CH300	2359-2391 (S)	5´-GAATAGGGGGAAACgcAgcGGTAAGATATCCGT-3´		pET-p12(1-59)mut2R
CH301	2359-2391 (AS)	5´-ACGGATATCTTACCgcTgcGTTTCCCCCTATTC-3´		
CH302	2370-2396 (S)	5´-AACgcAgcGGTAgcATATCCGTCGCAA-3´		pET-p12(1-59)mut3R
CH303	2370-2396 (AS)	5´-TTGCGACGGATATgcTACCgcTgcGTT-3´		
CH304	2385-2411 (S)	5´-TATCCGTCGCAAgcGACGCTGTCTCCA-3´		pET-p12(1-59)mut4R
CH305	2385-2411 (AS)	5´-TGGAGACAGCGTCgcTTGCGACGGATA-3´		

ᵃ Positions of the PFBV genome covered by the primers. (S) and (AS): sense and antisense.

ᵇ Restriction sites introduced for cloning purposes are underlined and lowercase indicate nucleotide substitutions to PFBV wt sequence.
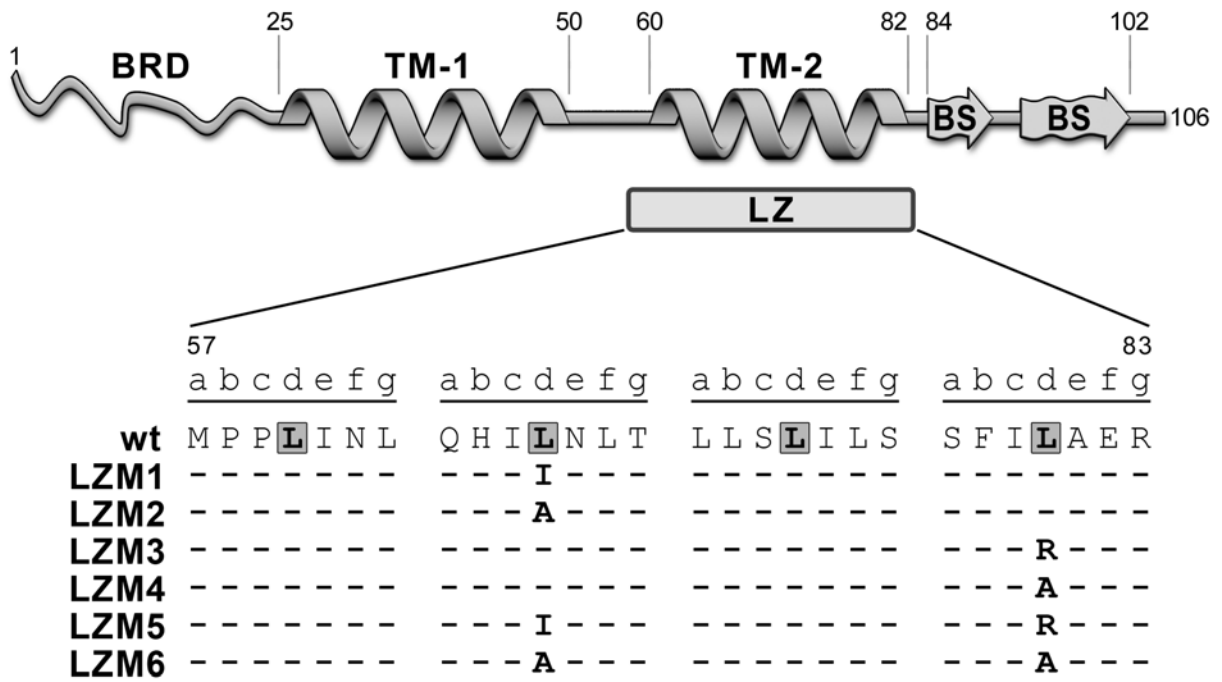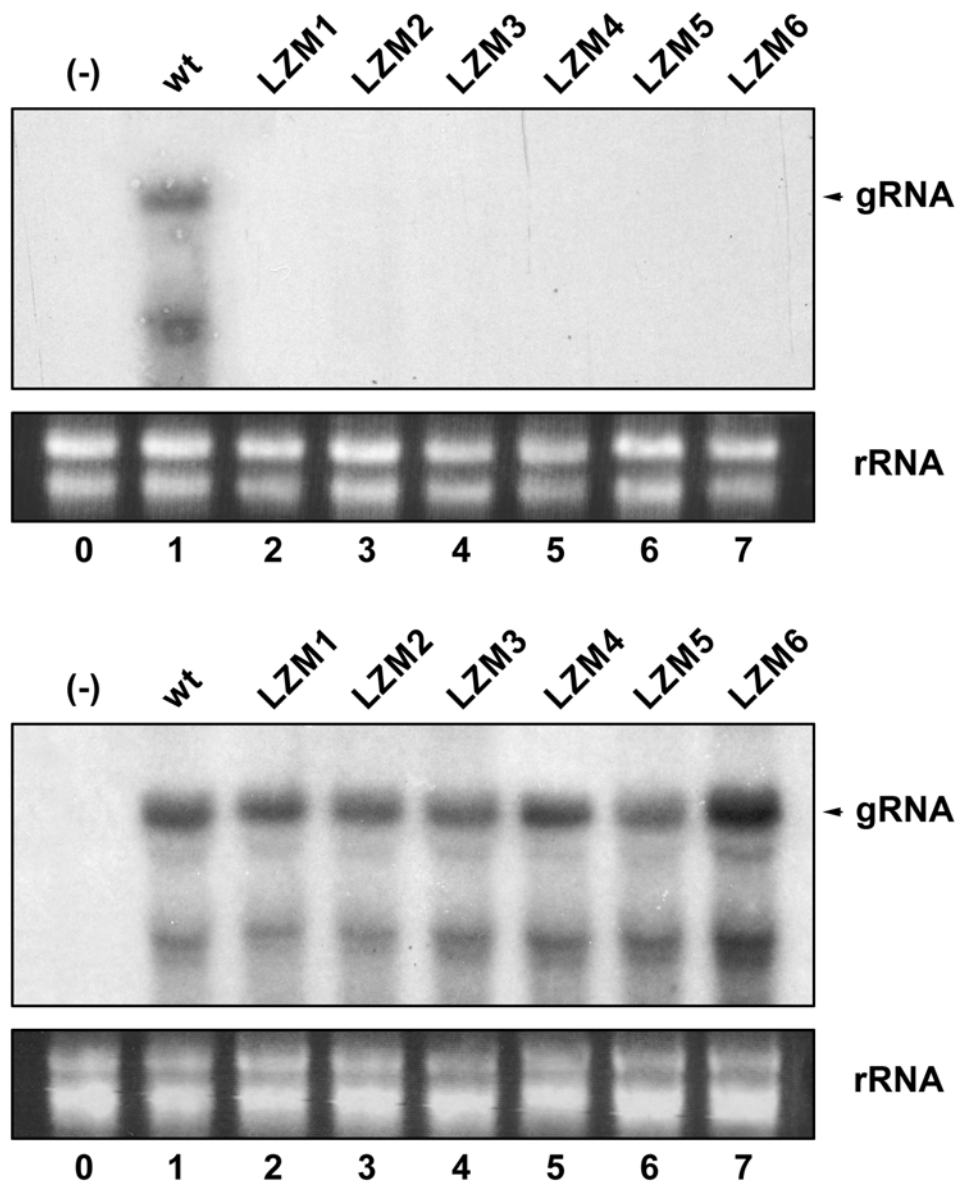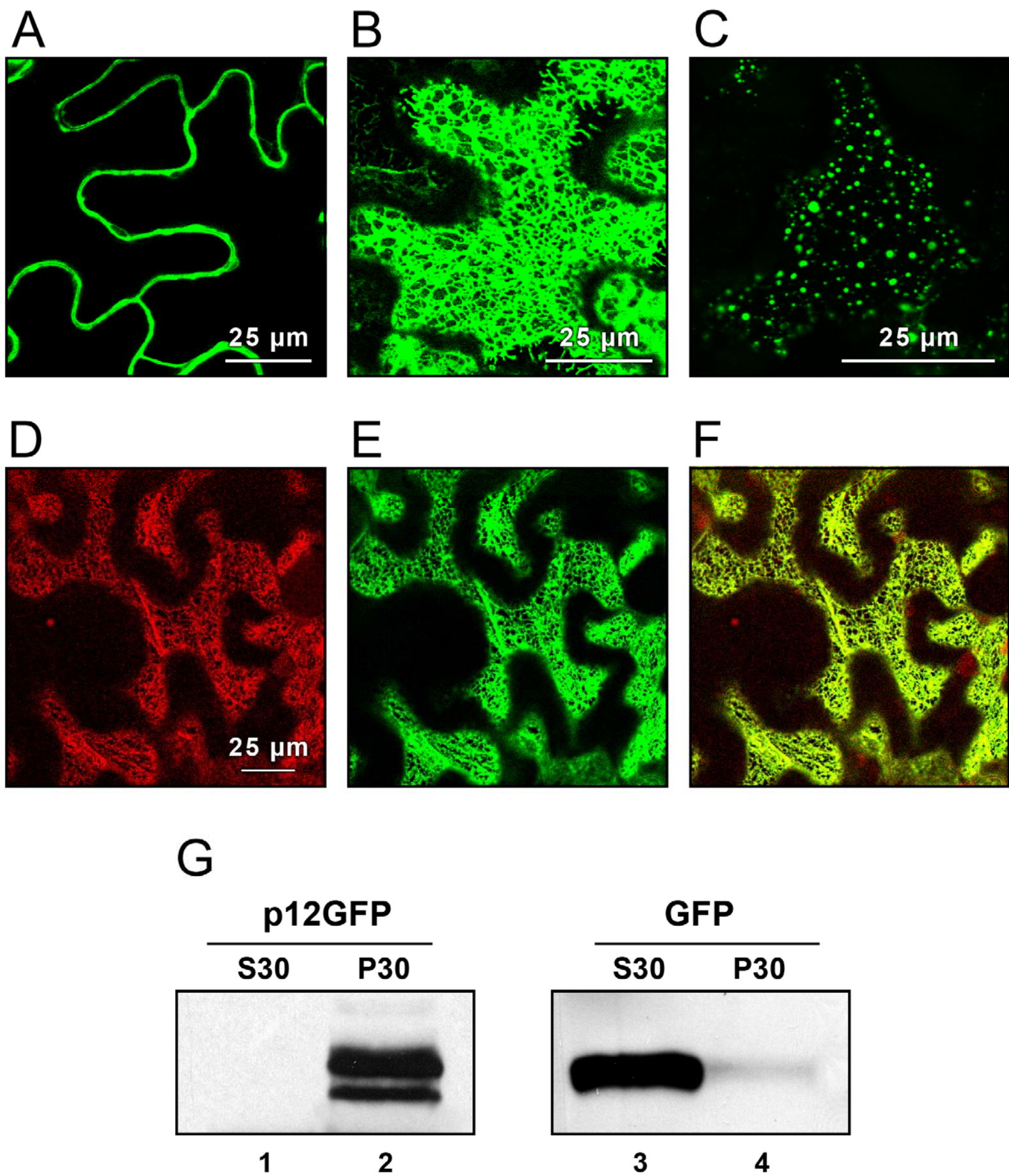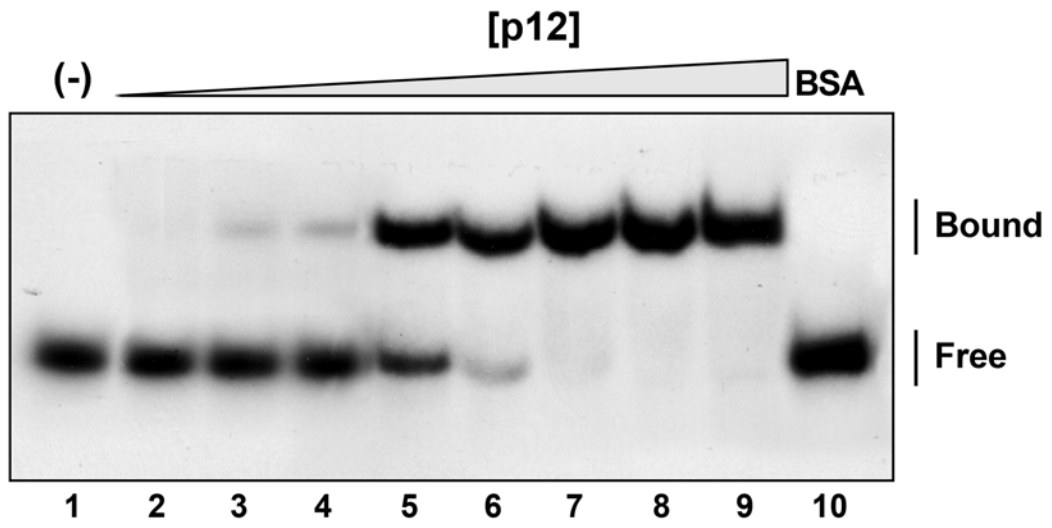
Fig. 1

Fig. 2

A

B

C

25 µm

25 µm

25 µm

D

E

F

25 µm

G

p12GFP

GFP

S30

P30

S30

P30

1

2

3

4

Fig. 3

A

(-)   [p12]   BSA

Bound

Free

1   2   3   4   5   6   7   8   9   10

B

Bound RNA (%) vs [p12] (μM)

C

Bound RNA (%) vs Log[NaCl] (mM)

Fig. 4

Fig. 5

A

p12 — 1 ... 106

p12 (26 - 106) — 1 ... 26 ... 106

p12 (1 - 59) — 1 ... R R R   R ... 59 ... 106

p12 (1 - 59) m2R — 1 ... * * A A R R ... 59 ... 106

p12 (1 - 59) m3R — 1 ... * * * A A A R ... 59 ... 106

p12 (1 - 59) m4R — 1 ... * * * * A A A A ... 59 ... 106

B

SDS-PAGE

NORTHWESTERN

p12 | p12 (26 - 106) | p12 (1 - 59) | p12 (1 - 59) m2R | p12 (1 - 59) m3R | p12 (1 - 59) m4R

kDa
49.5
37.4
26.0
20.5
14.9
8.4

Fig. 6